

**STRUCTURAL, OPTICAL AND THERMAL
PROPERTIES OF AINB MULTILAYER
COMPOSITE VIA STACKING METHOD FOR
LED THERMAL APPLICATION**

ABDULKARIM HAMZA EL LADAN

UNIVERSITI SAINS MALAYSIA

2023

**STRUCTURAL, OPTICAL AND THERMAL
PROPERTIES OF AINB MULTILAYER
COMPOSITE VIA STACKING METHOD FOR
LED THERMAL APPLICATION**

by

ABDULKARIM HAMZA EL LADAN

**Thesis submitted in fulfilment of the requirements
for the degree of
Doctor of Philosophy**

January 2023

ACKNOWLEDGEMENT

I hereby express my sincere gratitude and appreciation to Allah (SWT) for giving me endless help and opportunities to complete my research work and thesis. I will also express my sincere appreciation to my able, fast and hardworking supervisor Dr Shanmugan Subramani, for his motivation, guidance as well as perseverance and tolerance throughout my entire research work. I will also send my sincere gratitude to my co-supervisor Dr Mohd. Zamir Pakhurddin for his guidance and valuable inputs in the research work. I also acknowledge the contributions of my former supervisors, Prof Dr Fauziah Binti Sulaiman and Prof Dr Mutharasu Devarajan as well as all laboratory staffs from both the Thermal Management Research lab (TMRL) and Nano Optoelectronics Research Laboratory (NOR) for their supports. To my fellow research colleagues Idris, Muna, Anitha, Dheephan, Aida, Nabihah, Mutawalli, Vishnu, Murali, Vignesh and Puurnaraj, I will say thank you so much for your help and friendliness.

Finally, my special prayers and appreciation goes to my carering, loving and motivating late parents and the entire El-ladans family for their support and patience.

TABLE OF CONTENTS

ACKNOWLEDGEMENT	ii
TABLE OF CONTENTS	iii
LIST OF TABLES	ix
LIST OF FIGURES	x
LIST OF SYMBOLS	xv
LIST OF ABBREVIATIONS	xvii
LIST OF APPENDICES	xx
ABSTRAK	xxi
ABSTRACT	xxiii
CHAPTER 1 INTRODUCTION	1
1.1 Research Background.....	1
1.2 Thermal management of LED.....	4
1.3 AlN/B composite.....	7
1.4 Problem Statement	8
1.5 Research Objectives	9
1.6 Research Contributions	10
1.7 Research Novelty	11
1.8 Thesis Structure.....	12
CHAPTER 2 LITERATURE REVIEW	14
2.1 Introduction	14
2.2 Thermal management.....	16
2.2.1 Solid Thermal Interface Material	18
2.2.2 Influence of Thermal Interface Materials on Heat Mitigation	19
2.3 Overview of base material (BN) growth.....	21

2.3.1	Physical vapour deposition (PVD) techniques.....	24
2.3.2	Chemical vapour deposition (CVD) techniques	24
2.4	Overview of base material (AlN) growth.....	24
2.4.1	Significance of AlN.....	24
2.5	Overview of AlNB Growth.....	27
2.5.1	Formation of AlNB heterostructure by sputtering technique.....	32
2.5.2	Effect of varying layer thickness on the AlNB films.....	33
2.6	Theoretical background.....	33
2.6.1	Theory of Heat Transfer Through Solid Thermal Interface Materials.....	33
2.6.2	Thermal resistance	34
2.6.3	Contact resistance.....	34
2.6.4	Thermal impedance.....	35
2.6.5	Junction temperature	36
2.6.6	Derating curve.....	36
CHAPTER 3 METHODOLOGY		37
3.1	Introduction	37
3.2	Preparation of substrates	38
3.3	Deposition of thickness composite I ($Al_{1-x}NB_x$), II (AlNB) and III (BAlN)	39
3.3.1	Thickness composite I (Al/ $Al_{1-x}NB_x$)	40
3.3.2	Thickness composite II (Al/AlNB).....	41
3.3.3	Thickness composite III (Al/BAlN).....	42
3.3.4	Annealing	43
3.4	Material Characterization Techniques	43
3.4.1	Field Emission Scanning Electron Microscope (FESEM).....	43
3.4.2	Atomic Force Microscope (AFM)	44

3.4.3	X-ray diffractometer (XRD)	44
3.4.4	Fourier Transform Infrared (FTIR).....	45
3.4.5	Thermal Transient Tester (T3ster)	46
3.4.6	Thermal, Radiometric and Photometric Testing of LEDs using TeraLED	49
3.4.7	Derating curve Analysis of LEDs using TeraLED	51
3.5	Optical parameters	52
3.5.1	Luminous flux	52
3.5.2	Luminous efficacy.....	53

CHAPTER 4 RESULTS AND DISCUSSION

ANALYSIS OF AlNB COMPOSITE ON ALUMINIUM SUBSTRATE..... 54

4.1	Introduction	54
4.2	Characterizations of <i>AlNB</i> ($Al_{0.8}NB_{0.2}$) Nanocomposite Thin Film on Al Substrates with varied Gas Ratios.....	54
4.2.1	Surface Characterization of <i>AlNB</i> Nanocomposite	55
4.2.1(a)	Surface Morphology Analysis of <i>AlNB</i>	55
4.2.1(b)	Surface Roughness Analysis of <i>AlNB</i>	57
4.2.2	Phase Structure Analysis of <i>AlNB</i> Nanocomposite.....	59
4.2.3	Molecular Structural Analysis of <i>AlNB</i> Nanocomposite	63
4.2.4	Thermal Transient Analysis of <i>AlNB</i> Nanocomposite	64
4.3	Characterization of <i>AlNB</i> Nanocomposite Thin Film on Al Substrates with varied thickness ratios	65
4.3.1	Surface Characterization of $Al_{1-x}NB_x$ Nanocomposite	66
4.3.1(a)	Surface and Cross-Sectional Morphology Analysis of $Al_{1-x}NB_x$	66
4.3.1(b)	Surface Roughness Analysis of $Al_{1-x}NB_x$	71
4.3.2	Phase Structure Analysis of $Al_{1-x}NB_x$ Nanocomposite.....	72

4.3.3	Molecular Structural Analysis of $Al_{1-x}NB_x$ Nanocomposite	75
4.3.4	Thermal Transient Analysis of $Al_{1-x}NB_x$ Nanocomposite	76
4.4	Characterization of Al/NB Nanocomposite Thin Film on Al Substrates with varied stacking configurations ($Al/AlN/B$).....	77
4.4.1	Surface Characterization of AlN/B Nanocomposite.....	78
4.4.1(a)	Surface and Cross-Sectional Morphology Analysis of AlN/B	78
4.4.1(b)	Surface Roughness Analysis of AlN/B Nanocomposite.....	80
4.4.2	Phase Structure Analysis of Al/NB Nanocomposite.....	82
4.4.3	Molecular Structural Analysis of Al/NB Nanocomposite	85
4.4.4	Thermal Transient Analysis of Al/NB Nanocomposite.....	86
4.5	Characterizations of $BAlN$ Nanocomposite Thin Film on Al Substrates with varied stack configurations ($Al/B/AlN$).....	87
4.5.1	Surface Characterization of B/AlN Nanocomposite.....	88
4.5.1(a)	Surface and Cross-Sectional Morphology Analysis of B/AlN	88
4.5.1(b)	Surface Roughness Analysis of $BAlN$	91
4.5.2	Phase Structure Analysis of $BAlN$ Nanocomposite.....	92
4.5.3	Molecular Structural Analysis of $BAlN$ with Varied Stacking.....	94
4.5.4	Thermal Transient Analysis of $BAlN$ Nanocomposite.....	95
4.6	Summary	96

CHAPTER 5 RESULTS AND DISCUSSION

	THERMAL AND OPTICAL ANALYSIS OF WHITE BASED HIGH POWER (LED) ON AL (5052) SUBSTRATE COATED WITH OPTIMISED COMPOSITES I (e), II (i) and III (m)	100
5.1	Introduction.....	100
5.2	Thermal Analysis (Z_{th} , T_j and Derating curve) for LED fixed on Composite I (e).....	101

5.2.1	Thermal Impedance (Z_{th}) of LED fixed on composite I (e)	101
5.2.2	Rise in Junction Temperature (T_j) of LED fixed on composite I (e).....	102
5.2.3	Derating Curve for LED fixed on composite I (e)	103
5.3	Thermal Analysis (Z_{th} , T_j and Derating curve) for LED fixed on Composite II (i).....	105
5.3.1	Thermal Impedance (Z_{th}) of LED fixed on composite II (i)	104
5.3.2	Rise in Junction Temperature (T_j) of LED fixed on composite II (i).....	106
5.3.3	Derating Curve Analysis for LED fixed on composite II (i)	106
5.4	Thermal Analysis (Z_{th} , T_j and Derating curve) for LED fixed on Composite (III).....	108
5.4.1	Thermal Impedance (Z_{th}) of LED fixed on composite III (m)	108
5.4.2	Rise in Junction Temperature (T_j) of LED fixed on composite III (m).....	109
5.4.3	Derating Curve for LED fixed on composite III (i)	110
5.5	The Combine Thermal Performances (Z_{th} , T_j) for LEDs fixed on Composites I (e), II (i) and III (m)	112
5.5.1	Combine Thermal Impedance for LEDs on Composites I(e), II(i) and III(m).....	112
5.5.2	Combine Temperature Rise for LEDs on composite I(e), II(i) and III(m)	112
5.6	Optical Performance (Flux and Efficacy) of LEDs fixed on Composites I(e), II(i) and III(m) for comparison with manufacturers Data Sheet	114
5.6.1	Luminous Flux and Luminous Efficacy of LED fixed on composite I(e).....	114
5.6.2	Luminous Flux and Luminous Efficacy of LED fixed on composite II(i).....	115
5.6.3	Luminous Flux and Luminous Efficacy of LED fixed on composite III(m).....	116
5.7	Summary	117

CHAPTER 6 CONCLUSION AND RECOMMENDATIONS FOR FUTURE WORK	119
6.1 Conclusion	119
6.2 Recommendations for Future Research	120
REFERENCES	121
APPENDICES	
LIST OF PUBLICATIONS	

LIST OF TABLES

	Page
Table 2.1	Light source with approximate input power conversion to heat and radiant energy15
Table 2.2	Summary of previous works in thermal resistance and junction temperature reduction for grown TIMs from literatures.....20
Table 2.3	Summary of AlNB growth parameters and performance from literatures.....28
Table 4.1	Roughness Values of AlNB with varied gas ratios59
Table 4.2	AlN (200, 220, 111, 311) and Al (200, 220, 111, 311) d-spacing values based on XRD data base and JCPDS card no.....62
Table 4.3	Roughness Values of AlNB with varied thickness ratios72
Table 4.4	Roughness Values of AlNB for varied stacking sequence of AlN to B.....82
Table 4.5	Roughness Values of Samples (1-n) AlNB for varied stacking sequence of AlN to B.....92
Table 4.6	Important Results/Characteristics of the Optimized samples.....98

LIST OF FIGURES

		Page
Figure 1.1	Typical luminous efficacy of residential lighting in the Sustainable Development Scenario, 2010-2030 [7].....	2
Figure 1.2	Lighting sales by type in the Sustainable Development Scenario, 2010-2030 [7]	3
Figure 1.3	(a) Direct contact between LED package and heat sink (b) Contact between LED Package and Heat Sink via STIM.....	5
Figure 1.4	Measured reduction in Z_{th} (a) and T_j (b) of bare and composite I coated Al substrates at 700 mA.	10
Figure 2.1	Useful life of high-power LED at different operational temperatures.....	15
Figure 2.2	Heat flow path with one dimensional R_{th} model for the golden dragon LED	17
Figure 2.3	Schematic representing a real TIM and associated temperature distribution with resistor model [33]	19
Figure 2.4	Thermal contact resistance of heat source A and Heat dissipator B [136].....	35
Figure 2.5	Derating Curve of load vs operational temperature.....	36
Figure 3.1	Research methodology flow chart	38
Figure 3.2	Schematic representation of sputtered AlN/BN based on thickness ratios of Al and B ($Al_{1-x}NB_x$) e ($Al_{0.8}NB_{0.2}$), f ($Al_{0.6}NB_{0.4}$), g ($Al_{0.4}NB_{0.6}$), and h ($Al_{0.2}NB_{0.8}$).....	41
Figure 3.3	Schematic representation of three grown composites based on thickness ratio of AlN:B (100:10) nm.	42
Figure 3.4	Schematic representation of three grown composites based on thickness ratio of B:AlN (10:100) nm.	42
Figure 3.5	Experimental set up for the DUT with T3ster system showing (a) cold plate surface (b) commercial thermal pad fixed to the cold plate (c) Coated substrate attached to the cold plate via commercial thermal pad and (d) complete cold plate unit (DUT, Thermal Pad) covered with 1 bar spring-loaded cap.	48

Figure 3.6	K - factor graph for high power white LED	49
Figure 3.7	Experimental set up for the DUT with TeraLED system showing (a) temperature stabilized LED fixture surface (b) commercial thermal pad fixed to the temperature stabilized LED fixture surface (c) Coated substrate attached to the temperature stabilized LED fixture via commercial thermal pad and (d) complete temperature stabilized LED fixture unit (DUT, Thermal Pad) covered with Screwed Cap at (1 bar).....	51
Figure 3.8	Derating Curve of load vs operational temperature.....	52
Figure 4.1	(a-d) FESEM Photomicrograph of $Al_{0.8}NB_{0.2}$ thin film with varied gas ratios	55
Figure 4.2	(a-d) 3D Surface Topography of AlNB with varied gas ratios	59
Figure 4.3(a)	XRD pattern of AlN and Al of AlNB with varied gas ratios.....	61
Figure 4.3(b)	Expanded view of BN XRD pattern of AlNB with varied gas ratios	61
Figure 4.3(c)	Expanded view of XRD pattern for (220) diffraction peak of AlNB with varied gas ratios.....	63
Figure 4.4	IR Transflectance Spectra of AlN and BN of AlNB based on Al and B sputtering targets with varied gas ratios.....	64
Figure 4.5	Cumulative Structure Function for High Power LED mounted on AlNB (with varied gas ratios) coated and uncoated substrates at 300mA.	65
Figure 4.6	(e-h) FESEM Photomicrograph of $Al_{1-x}NB_x$ composite with varied thickness ratios (Al and B targets).....	68
Figure 4.7	(e-h) FESEM Photomicrograph of $Al_{1-x}NB_x$ composite with varied thickness ratios tilted at 30°	69
Figure 4.8	(e-h) FESEM Cross-sectional Photomicrograph of $Al_{1-x}NB_x$ composite with varied thickness ratios	70
Figure 4.9	(e-h) 3D AFM Surface Topography of $Al_{1-x}NB_x$ with varied thickness ratios	72
Figure 4.10	XRD spectra of ($Al_{1-x}NB_x$) with varied thickness ratios	74
Figure 4.11	Expanded view of XRD spectra for (220) diffraction peak with varied thickness ratios.....	74

Figure 4.12	IR Transflectance Spectra of AlN and BN of Al _{1-x} NB _x composite with varied thickness ratios	75
Figure 4.13	Cumulative Structure Function for High Power LED mounted on AlNB (with varied thickness ratios) coated and uncoated substrates recorded at 300mA	76
Figure 4.14	(i-k) FESEM Photomicrograph of AlNB prepared with varied stacking sequence of AlN and B.....	79
Figure 4.15	(i-k) FESEM Photomicrograph of AlNB with varied stacking sequence of AlN to B at tilt angle of 30°	79
Figure 4.16	FESEM Cross-Sectional Photomicrograph of AlNB composite with varied stacking sequence of AlN and B.....	80
Figure 4.17	3D AFM Surface Topography of AlNB for varied stacking sequence of AlN to B	82
Figure 4.18	XRD pattern of AlNB composite for varied stacking sequence of AlN and B	84
Figure 4.19	Expanded view of XRD pattern for (220) diffraction peak of AlN and AlNB with AlN/B stacking sequence	84
Figure 4.20	IR Transflectance Spectra of AlN B composite with varied stacking sequence of AlN and B	85
Figure 4.21	Cumulative Structure Function for High Power LED mounted on AlNB with varied stacking sequence coated and uncoated substrates at 300mA.....	87
Figure 4.22	(l-n) FESEM Photomicrograph of BAlN with varied stacking sequence of B to AlN.....	90
Figure 4.23	FESEM Photomicrograph of BAlN with varied stacking sequence at tilt angle of 30°	90
Figure 4.24	FESEM Cross-Sectional Photomicrograph of BAlN with varied stacking sequence of B to AlN	90
Figure 4.25	3D AFM Surface Topography of BAlN for Varied Stacking sequence.....	92
Figure 4.26	XRD spectra of BAlN composite for varied stacking sequence of B to AlN	93
Figure 4.27	Expanded BAlN XRD spectra for (220) diffraction peak for varied stacking sequence of B to AlN	94

Figure 4.28	IR Transflectance Spectra of AlN and BN with varied stacking sequence of B to AlN.....	95
Figure 4.29	Cumulative Structure Function for High Power LED mounted on BAlN with varied stacking sequence coated and uncoated substrates at 300mA	96
Figure 5.1	Thermal impedance of LED fixed on bare and composite I(e) coated Al substrate at 300 and 700 mA	101
Figure 5.2	Junction Temperature rise of LED fixed on bare and composite I(e) coated Al substrates at 300 and 700 mA	102
Figure 5.3	Derating curve for LED fixed on bare and composite I(e) coated Al substrates at 0 - 1050 mA	104
Figure 5.4	Histogram for operational temperature of LED fixed on bare and composite I(e) coated Al substrate at 0 - 1050 mA	104
Figure 5.5	Thermal impedance of LED fixed on bare and composite II(i) coated Al substrates at 300 and 700 mA	105
Figure 5.6	Junction Temperature rise of LED fixed on bare and composite II(i) coated Al substrates at 300 and 700 mA	106
Figure 5.7	Derating curve for LED fixed on bare and composite II(i) coated Al substrates at 0 - 1050 mA.....	107
Figure 5.8	Histogram for operational temperature of LED fixed on bare and composite II(i) coated Al substrates at 0 - 1050 mA.....	108
Figure 5.9	Thermal impedance of LED fixed on bare and composite III(m) coated Al substrates at 300 and 700 mA	109
Figure 5.10	Junction Temperature rise of LED fixed on bare and composite III(m) coated Al substrates at 300 and 700 mA.....	110
Figure 5.11	Derating curve for LED fixed on bare and composite III(m) coated Al substrates at 0 - 1050 mA	111
Figure 5.12	Histogram for operational temperature of LED fixed on bare and composite III(m) coated Al substrates at 0 - 1050 mA.....	111
Figure 5.13	Combine Thermal impedance of LEDs on composite I(e), II(i) and III(m) coated substrates at 300 and 700 mA.....	112
Figure 5.14	Combine Temperature Rise of LEDs on composite I(e), II(i) and III(m) coated substrates at 300 and 700 mA.....	113

Figure 5.15	Compared Luminous flux and Efficacy of LED fixed on composite I(e) with manufacturers data sheet.....	115
Figure 5.16	Compared Luminous flux and Efficacy of LED fixed on composite II(i) with manufacturers data sheet	116
Figure 5.17	Compared Luminous flux and Efficacy of LED fixed on composite III(m) with manufacturers data sheet.....	117

LIST OF SYMBOLS

A	Cross-sectional area
\AA	Angstrom
cm	Centimetre
ε	Microstrain
D	Crystallite Size
c	Cubic
$^{\circ}\text{C}$	Degree Celsius
d	Diffraction Spacing
δ	Dislocation Density
eV	Electron Volt
h	Hexagonal
Hz	Hertz
I	Current
Kg	kilogram
J	Joule
lm	Lumen
lm/w	Luminous Efficacy
mA	Milliampere
Mbar	Millibar
nm	Nanometer
%	percentage
Ω	Ohm
Pa	Pascal
Q	Heat Source

q	Total Heat Flux
R	Resistor
R_{th}	Thermal resistance
$R_{th(j-a)}$	Thermal Resistance from Junction to Ambient
$R_{th c}$	Contact Resistance
ΔR_{th}	Difference in Thermal Resistance
T	Time
θ	Differential Angle
λ	Wavelength
T_j	Junction Temperature
T_{2A}	Temperature of Device
T_{2B}	Temperature of Heat Sink
T_a	Ambient Temperature
P_d	Power Dissipated
V	Voltage
W	Watt
Z_{th}	Thermal Impedance
$Z_{th(j-a)}$	Thermal Impedance from Junction to Ambient

LIST OF ABBREVIATIONS

AFM	Atomic Force Microscope
AAO	Anodise Aluminium Oxide
Al	Aluminium
AlN	Aluminium Nitride
AlNB	Aluminum Nitride Boron
Al ₂ O ₂	Aluminium Oxide
Ar	Argon
ASTM	American Society for Testing and Materials
B	Boron
BAlN	Boron Aluminium Nitride
BeO	Beryllium Oxide
BLT	Bond Line Thickness
BN	Boron Nitride
CFL	Compact Fluorescent Lamp
CO ₂	Carbon Dioxide
CVD	Chemical Vapor Deposition
3D	Three dimensional
DC	Direct Current
DOE	Department of Energy
DSP	Density of Peaks
DUT	Device Under Test
EDX	Energy Dispersive X-Ray
FESEM	Field Emission Scanning Electron Microscope
FL	fluorescent

FME	Flow-Modulate Epitaxy
FTIR	Fourier-transform infrared spectroscopy
GHG	Green House Gas
H	Hydrogen
HID	High-Intensity Discharge
HCl	Hydrochloric Acid
HF	Hydroflouric Acid
H ₂ O	Water
H ₂ O ₂	Hydrogen Peroxide
IBAD	Ion Beam Assisted Deposition
ICDD	International Center for Diffraction Data
IEA	International Energy Agency
IR	Infrared
JCPDS	Joint Committee On Power Diffraction Standards
JEDEC	Joint Electron Device Engineering Council
LED	Light Emitting Diode
MBE	Molecular Beam Epitaxy
MCPCB	Metal Core Printed Circuit Board
MEMS	Micro Electromechanical Systems
MgO	Magnesium Oxide
MOCVD	Metal Organic Chemical Vapor Deposition
MOVPE	Metal-Organic Vapor Phase Epitaxy
N	Nitrogen
NH ₃	Ammonia
Ni	Nikel
NOR	Nano Optoelectronics Research Laboratory

OMVPE	Organometallic Vapor-Phase Epitaxy
PCB	Printed Circuit Board
PCM	Phase Change Material
PECVD	Plasma-Enhanced Chemical Vapour Deposition
PLD	Pulsed Laser Deposition
PVD	Physical Vapor Deposition
RCA	Radio Corporation of America
RF	Radio Frequency
RMS	Root Mean Square
RPM	Revolution Per Minute
SDS	Sustainable Development Scenarios
Si	Silicon
SI	International System of Units
SSL	Solid State Light
3D	Three Dimensional
STIM	Solid Thermal Interface Material
SCCM	Standard Cubic Centimeter Per Minute
TIM	Thermal Interface Materials
TMRL	Thermal Management Research laboratory
TeraLED	Thermal, Radiometric and Photometric Testing
T3ster	Thermal Transient Tester
UV	Ultraviolet
XRD	X-ray diffractometer
ZnO	Zinc Oxide

LIST OF APPENDICES

Appendix A	Golden Dragon Led Data Sheet
Appendix B	Thermal Transient Tester (T3Ster)
Appendix C	Thermal and Radiometric/Photometric Tester (TeraLED)
Appendix D	Summary of <i>B-N</i> and <i>Al-N</i> Bondings from Literature
Appendix E	Summary XRD Reflection Peaks for <i>BN</i> and <i>AlN</i> from Literature

SIFAT STRUKTUR, OPTIK DAN TERMA KOMPOSIT ALNB BERBILANG LAPIS MELALUI KAEDAH SUSUNAN UNTUK APLIKASI TERMA LED

ABSTRAK

Permintaan berterusan untuk diod pemancar cahaya (LED) semakin meningkat kerana ia merupakan pilihan yang baik berbanding lampu pijar, pendarfluor (FL, CFL) dan lampu halogen yang tidak cekap. Walau bagaimanapun, prestasi, kebolehpercayaan dan hayat operasi LED dipengaruhi oleh pengumpulan haba yang berlebihan di dalam LED, oleh itu, keperluan untuk membangunkan bahan rintangan haba rendah (R_{th}) sebagai bahan termal antara muka (STIM) yang unik, teguh dan serba boleh amat perlu ditekankan. Dalam kerja penyelidikan ini, filem nipis komposit nano AlNB disintesis menggunakan teknik percikan reaktif ke atas substrat aluminium dan analisis terhadap prestasi (terma/optik) LED yang dipasang pada komposit yang telah dibina dijalankan. Sintesis dijalankan dalam tiga konfigurasi berbeza yang dinamakan sebagai komposit (I, II dan III). Komposit dibina berdasarkan sasaran Al dan B dengan nisbah ketebalan yang berbeza menggunakan empat nisbah gas ($N_2:Ar$) berbeza dan suhu penyepuhlindapan ($200-400^\circ C$), manakala komposit (II dan III) adalah berdasarkan sasaran AlN dan B dengan ketebalan tetap nisbah dalam tiga susun atur yang berbeza, nisbah gas ditetapkan sebagai 12:8 dan suhu penyepuhlindapan ditetapkan sebagai $400^\circ C$. Pencirian struktur dikaji menggunakan difraktometer sinar-X beresolusi tinggi (XRD) dan mengesahkan kehadiran (225) fasa c -AlN, (216) fasa c -BN dan (216) fasa struktur c -Al, Fasa c -AlN dan c -BN disahkan lagi oleh spektrum trans-pantulan daripada Fourier transform infrared spectroscopy (FTIR) antara ~ 512 dan 1672 cm^{-1} . Menggunakan Atomic Force Microscopy (AFM) dan Field emission scanning electron microscope (FESEM), zarah nano bertaburan dengan saiz purata 80

– 200 nm dan retak bersaiz nano ~300 nm diperhatikan dalam komposit (I), manakala saiz 80 – 300 nm dan 80 – 220 nm nanozarah diedarkan dalam komposit (II dan III) masing-masing. Kekasaran permukaan komposit dinilai dan direkodkan menggunakan perisian nanoskop dalam julat 82 – 227 nm, 54 – 82 nm dan 48 – 58 nm masing-masing untuk komposit (I, II dan III) yang merupakan petunjuk permukaan yang baik untuk meminimumkan sentuhan haba rintangan. Dengan menggunakan lengkung fana penyejukan dan analisis fungsi struktur kumulatif, (R_{th}) antara muka didapati ~1.76, 3.0 dan 1.78 K/W manakala kenaikan suhu simpang (T_j) berdasarkan komposit (I-III) yang dibangunkan didapati jauh lebih rendah ~ 5.6, 7.2 dan 5.8°C berbanding substrat kosong dengan (9.77°C). Akhir sekali, peningkatan dalam prestasi optik (keberkesanan) berdasarkan komposit (I) menggantikan unjuran pertumbuhan keberkesanan global tahunan sebanyak 6 – 8 lm/W, ini menggambarkan kebaharuan kerja penyelidikan.

**STRUCTURAL, OPTICAL AND THERMAL PROPERTIES OF ALNB
MULTILAYER COMPOSITE VIA STACKING METHOD FOR LED
THERMAL APPLICATION**

ABSTRACT

The continuous demand for light-emitting diodes (LED) is increasing as it is a retrofitting option for in-efficient incandescent, fluorescent lights (FL, CFL) and halogen lamps. However, their performance, reliability, and operational life are affected by accumulation of excessive heat within the LED, thus, the need to develop a unique, robust, and versatile low thermal resistance (R_{th}) solid thermal interface material (STIM) cannot be over emphasized. In this research work, AlNB nanocomposite thin films are synthesized using reactive sputtering on aluminium substrates and performance analysis (thermal/optical) of LED mounted on the grown composites is conducted. The synthesis is carried out in three different configurations named as composites (I, II and III). Composite (I) is grown based on Al and B targets with varied thickness ratios using four different ($N_2:Ar$) gas ratios and annealing temperature (200-400°C), while composites (II and III) were based on AlN and B targets with fixed thickness ratios in three different stacking sequence at fixed gas ratio of 12:8 and annealing temperature of 400°C. The structural characterizations are studied using High-resolution X-ray diffractometer (XRD) and confirmed the presence of (225) phase of *c*-AlN, (216) phase of *c*-BN and (216) phase of *c*-Al structures. The *c*-AlN and *c*-BN phases are further confirmed by transmittance spectra from Fourier-transform infrared spectroscopy between ~ 512 and 1672 cm^{-1} . Using atomic force microscopy (AFM) and Field Emission Scanning Electron Microscopy (FESEM), scattered nanoparticles with average size of 80 – 200 nm and nano cracks of $\sim 300\text{nm}$

were observed in composite (I), while the distribution of 80 – 300 nm and 80 – 220 nm size nanoparticles are confirmed in composite (II and III) respectively. The surface roughness of the composites is evaluated and recorded using nanoscope software, in the range of 82 – 227 nm, 54 – 82 nm and 48 – 58 nm for composites (I, II and III) respectively, this is an indication of good surface quality which will intensively minimise thermal contact resistance. Using the cooling transient curve and cumulative structure function analysis, the interfacial R_{th} was found to be ~1.76, 3.0 and 1.78 K/W while the junction temperature (T_j) rise based on the developed composites I-III was found to be much lower ~5.6, 7.2 and 5.8°C compared to that of bare substrate (9.77°C). Finally, improvement in optical performance (efficacy) based on composite I supersedes the projected annual global efficacy growth of 6 – 8 lm/W, this portray the novelty of the research work.

CHAPTER 1

INTRODUCTION

1.1 Research Background

According to International Energy Agency (IEA) (2021), electricity demand is due to increase by 4.5% in 2021, which is believed to be the fastest growth in the last 10 years, cementing electricity's share in final energy demand above 20% [1]. However, 15% of global electricity use goes to lighting (residential, industrial and streets combine) corresponding to the combined electricity consumption of Russia, France, Australia, Indonesia, Germany and the UK [2]. In the past forty years, developed countries implement energy efficiency practices to serve as a large source of energy, reducing gas, oil and coal use to about 50%, directly lowering CO_2 emission and electricity cost [2].

Solid State Lights (SSL) most especially LEDs play an excellent role in saving energy which is translated into energy cost reduction, lower CO_2 emission and peak demand reduction, it also offers better service life with high lumen power at less wattage compared to inefficient incandescent bulbs, fluorescent lights (FL, CFL), High-Intensity Discharge (HID) and halogen lamps [3, 4]

LED-based lighting is expected to become the most dominant lighting technology of the future, surpassing all conventional lighting technologies driven by its edge with respect to service life, energy efficiency, versatility and lower cost [5, 6]. The luminous efficacy of LED is improving considerably in recent years, with an improvement of 6 – 8 lm/W per year since 2010 [7] and according to projections based

on sustainable development scenario (SDS), it will attain 161 lm/W by 2023, while the conventional lighting technologies, on the other hand, will not see improvement as indicated in Fig 1.1.

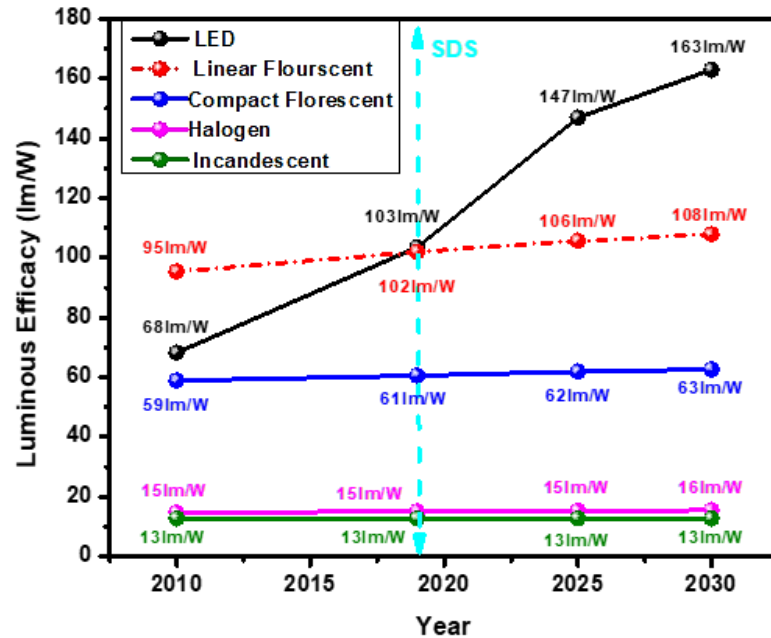


Figure 1.1 Typical Luminous Efficacy of Residential Lighting in the Sustainable Development Scenario, 2010-2030 [7]

The IEA (2020) report indicated that more than 10 billion units of LED in a form of bulbs, tubes, modules and luminaires were sold in 2019 across the globe, while the sales of conventional lighting technologies (fluorescent and others) are declining as indicated in Fig 1.2. The prices of LEDs are falling with the annual increase in efficacy and as well following the trend of the SDS projections to meet up with the 90% sales target by 2030 [7].

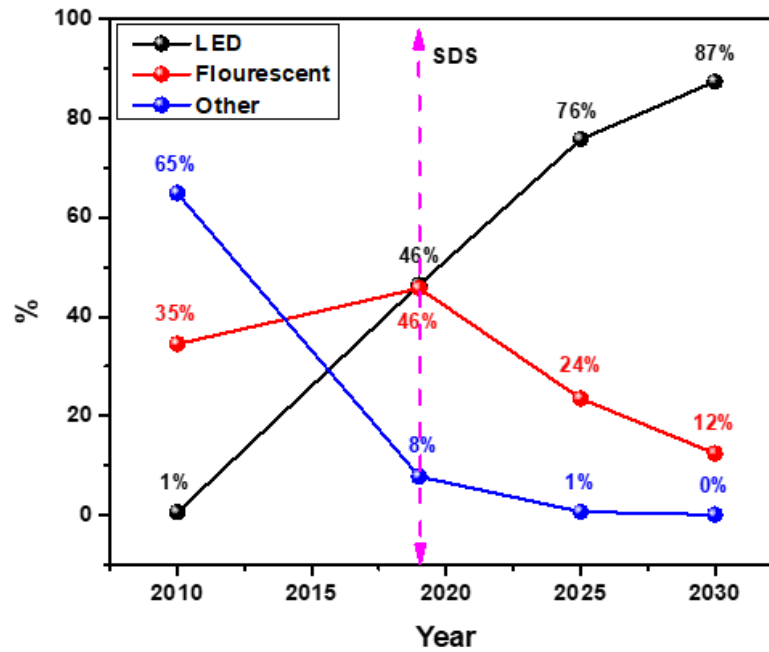


Figure 1.2 Lighting Sales by Type in the Sustainable Development Scenario, 2010-2030 [7]

Even though, the LED technology has attained a landmark in luminous efficacy and sales against the conventional technologies, however, for the technology to reach the projected efficacy and acceptability by 2030, it must overcome some challenges such as performance, reliability and operational life, which are largely driven by thermal path, ambient temperature and driving current.

LEDs and conventional light sources convert electrical power into radiant energy and heat in diverse proportions. Conventional light emits visible light, infrared IR, ultraviolet UV and heat, while LED emits visible light based on its luminous efficacy proportion and the remaining is converted to heat. On the other hand, the quest for higher flux delivery requires a higher driving current which in turn generate excessive heat at the die-attach leading to thermal fatigue, which in turn influences reduction in reliability and operational life [8]. The accumulated heat must be mitigated through the improvement of the thermal path, lower ambient temperature

and lower drive current for performance, reliability and operational life improvement of the LED [9,10].

1.2 Thermal Management of LED

The influence of thermal, electrical and optical characteristics of LEDs are interwoven with each other, but heat is considered to be one of the major influencing factor in lowering energy conversion efficiency in Solid State Light (SSL) [9]. The (T_j) must be mitigated within the safe operational limits of the LED to improve its performance through the modification of its thermal path by deploying either active or passive thermal management technique.

The active system is associated with higher cost due to the introduction of a fan and their operational power, on the other hand, the passive system is the most desired since it offers simple structure, requires no fan, low cost and is cheaper to maintain [11]. However, one of the biggest challenges in the passive system is the presence of uneven contact points and gaps created as a result of surface roughness between the LED package and the heat sink largely occupied by air creating high R_{th} and hence low heat transfer [12, 13].

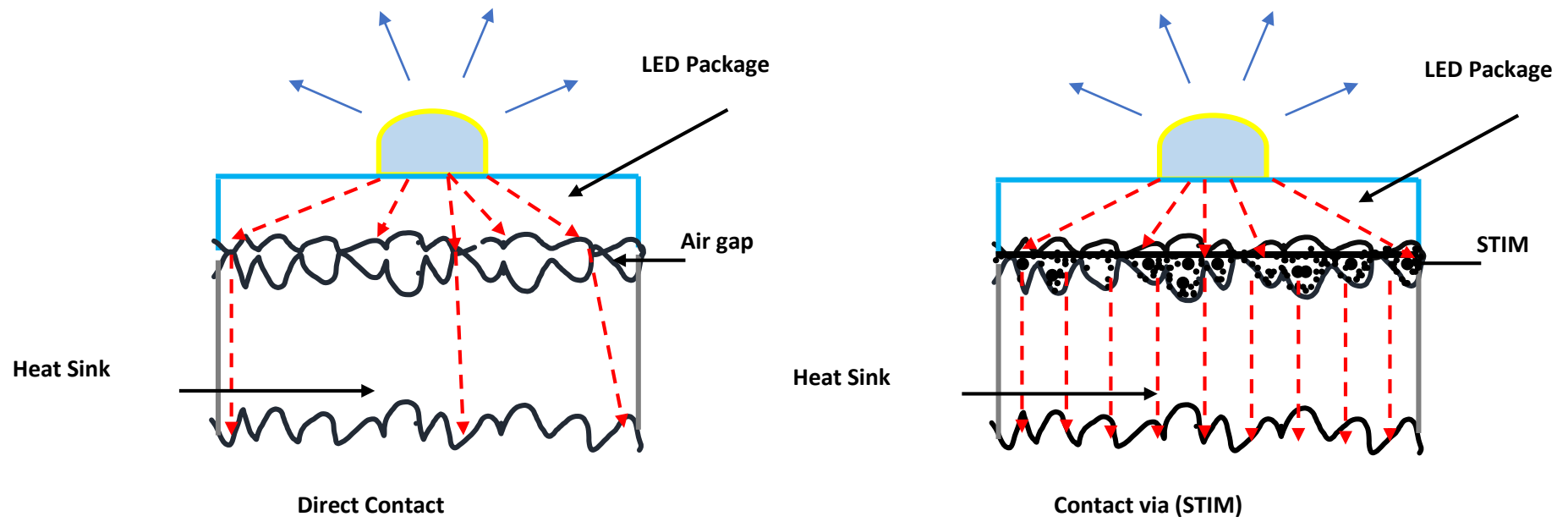


Figure 1.3 (a) Direct Contact between LED Package and Heat Sink (b) Contact between LED Package and Heat Sink via STIM

Thermal path improvement in the passive system is achieved through the surface of heat sink filling with low R_{th} materials in the form of pad, grease or STIM for the total or partial displacement of air in the gaps between the sink and LED surfaces as illustrated in Fig. 1.3.

Previous and current studies in thermal management have shown promising developments in STIM for passive thermal management applications using various base materials such as ZnO, MgO, Al₂O₃, AlN, BeO, BN grown with different techniques and analysed through thermal transient testing. The reported results are indicating a good reduction in R_{th} [12]

Some researchers chose materials such as AlN, BeO and BN with emphasis on low R_{th} or high thermal conductivity which are mostly associated with high cost and believed to be prospective materials in thermal management application due to their excellent thermal and mechanical properties, such as; high thermal conductivity (250 - 600 W/mK), low R_{th} , high melting point (2,530 - 2,973 °C) , low thermal expansion coefficient (8-1.2X10⁻⁶/K) , high electrical resistivity (10⁸ - 10¹⁷ Ω-cm) and high dielectric breakdown strength (330-800 volts/mil) [14-17], ability to operate at higher temperatures and other harsh conditions [16-20]. On the other hand, researchers consider other materials like MgO and ZnO for a trade-off between lower thermal performance with cost. Considering the global need for SSL for energy efficiency and CO₂ emission mitigation, there is a need to develop materials with excellent performance capabilities at a lower cost.

1.3 AlNB Composite

c-AlN and *c*-BN are unique and versatile ceramic compounds from group III-V with exciting properties such as excellent thermal and mechanical properties, wide bandgap of $\sim 5 - 6.2$ eV [2, 5], high electrical resistivity, high dielectric breakdown strength and high melting point which are prerequisite properties for thermal management applications [16, 17, 19, 20]. The qualities of both AlN and BN is making them good ceramic-based candidates to grow a well-balanced alloy material with high thermal conductivity, low R_{th} , low electrical conductivity and good processability in the thin-film form [11] for effective thermal management application in both low and high current densities or in high-power devices [16]

c-AlNB composite is a new material, developed from the base materials of *c*-AlN and *c*-BN using various techniques MOVPE, MBE, CVD, and Sputtering at different temperatures, pressure and gas ratios. The material is grown in the form of either Al or B rich alloy options and are currently being explored as novel members of the nitride III families for thermal management, optoelectronics and electronics applications. However, apart from theoretical investigations on the alloy, no much experimental explorations were carried out and presented in past literature, [10, 14, 16, 19] thus, further investigations in the growth and properties should be carried out by researchers.

Although it is challenging to grow the *c*-AlNB alloy with high crystal quality due to some intrinsic problems [16], however, boron and aluminium nitride with a cubic microstructure has higher thermal conductivity values (250–600 W/mK) than *h*-BN (29-300W/Mk) and *h*-AlN (50-220 W/Mk) [19, 21, 184]. This research work intends to present the fabrication details of *c*-AlNB alloy in three different stacking

configurations of Al/AlN_B, Al/BAlN and Al/Al_{1-x}NB_x thin film on aluminium substrates (to see the effect of super lattice sequence of the grown materials) on thermal management of LED, using radio frequency (RF) and (DC) reactive sputtering at room temperature and post annealed at 400°C. The low temperature annealing is carried out in nitrogen gas ambient for one hour, to increase in Al-N/B-N bond density as well as reduce surface roughness and residual stress [185, 105].

Further studies is carried out on the material's phase structure and molecular structure to establish the presence of components making up the composite, while surface morphology couple with surface topography analysis indicate clearly the surface quality of the composite which is pre requisite for effective thermal management beside the materials thermal properties, finally the thermal transient test, using cumulative structure function analysis is used to analyse and establish the possibility of using the alloy for effective thermal management as presented in the work. The consequential effects of the material on the optical performance of the LED and newly established operational parameters of the LED based on the developed material in relation to the operational parameters given by the manufacturers is presented [19]. Whereas, stacking of thin films by RF/DC reactive sputtering at room temperature and post-annealing is considered a new approach for the preparation of the alloy [22-24].

1.4 Problem Statement

Passive Thermal management of LED are expected to be revolutionized through the development of efficient dielectric nano materials from different base materials, for the mitigation of generated heat to improve the thermal path, however:

- The reduction in T_j of LED by the most grown materials from nitrides (AlN, BN) and oxides (ZnO, MgO, Al₂O₃) were below 10°C as reported in previous literatures.
- Commercially available TIMs (> 1 micron) such as thermal pad, paste, adhesive and thermal grease often dry and pump out, causing rise in junction temperature.
- The rise in T_j of the LED by 10°C would be reduced the 50% of useful life which increases the chances of thermal runaway as well as lower optical performance of the LED.
- Previous researchers rarely establish safe operational zone for LEDs based on developed thermal interface materials

1.5 Research Objectives

The main objectives of the research work are to:

- i. Develop, analyze and optimize the properties of the grown AlNB multilayer nanocomposites against the pure and thicker AlN, as a STIM on Al substrates for effective thermal management applications
- ii. Study the influence of the developed STIM (< 1 micron) in the improvement of the LED's total thermal resistance (R_{th}), thermal impedance (Z_{th}) and junction temperature (T_j)
- iii. Analyze the Improvement in the useful life, luminous flux and luminous efficacy of the STIM interfaced LED

- iv. Establish the safe operational zone for the LED before it gets derated based on the developed STIM

1.6 Research Contributions

This research work is geared towards improving the thermal and optical performance of solid-state lights (SSL) as indicated in figure 1.4 (a) and (b) through the development of robust composite material.

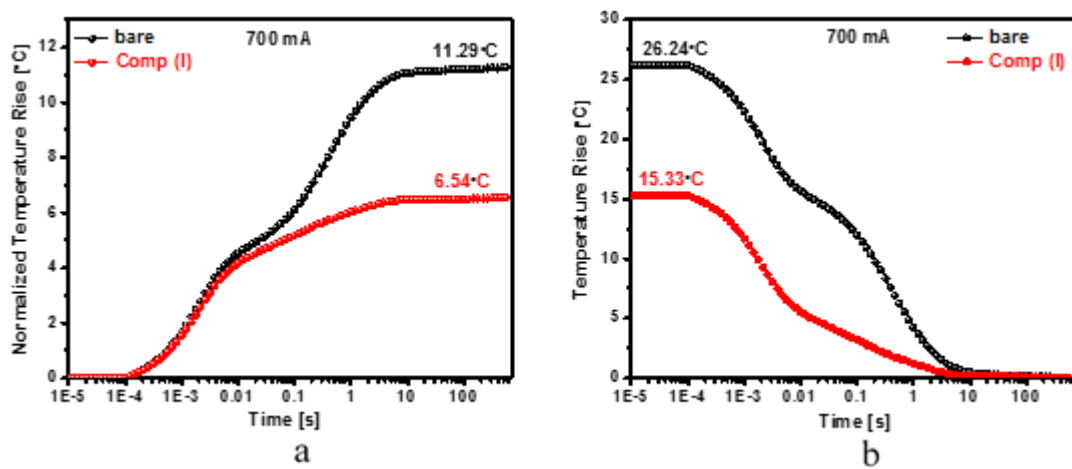


Figure 1.4 Measured Reduction in Z_{th} (a) and T_j (b) of Bare and Composite I Coated Al Substrates at 700 mA.

Fig 1.4(a) indicates ~ 40% reduction of Z_{th} and ~42% reduction of T_j (11°C) which are a noticeable achievement in LED performance and believe to improve the operational life of LED by over 50%.

The overall thermal performance of the LED package based on the coated substrate is improved greatly when compared with the uncoated substrate. Thus, the following contributions were made by the research work to improve the thermal and optical performance of the LED through:

The development of robust composite material with lower thickness and hence lowest R_{th}

- The reduction of total R_{th} and T_j of the LED package
- The improvement of the optical performance of the LED.
- The establishment of safe operational zone for the LED

1.7 Research Novelty

Variety of dielectric materials (oxides and nitrides) were developed by different researchers over the years, using different techniques and varied arrangements on different substrates towards mitigating T_j to improve thermal, optical and operational life of the LED.

However, attaining T_j mitigation over 10°C is becoming challenging to a lot of researchers and manufacturers, from our work presented herein, we were able to attain the following:

- Base on the arguments from previous literatures, the operational life of the LED is believed to improve by about 50% with the reduction of T_j to about 11°C in this work.
- The improvement in optical performance (luminous flux) to 100 lm against 85 lm at 350 mA and (luminous efficacy) to 108.6 lm/W against 99 lm/W from the data sheet is attained, the performance is observed to go beyond the desired global growth of 6-8 lm/W per year according to SDS [7].
- The safe operational temperature for the LED is believed to extend beyond the manufactures specification with the help of developed

composites (I, II and III) as STIM and proved by the derating curves in chapter 5.

1.8 Thesis Structure

The thesis is structured into six (6) chapters:

Chapter 1 – Introduction: This chapter dwells into the background of the study of LEDs performance compared to the conventional lighting technologies in the global market, it also introduces the thermal management of LEDs and an overview of AlNB nanocomposite. Furthermore, the motivation for the research work, the problem statement of the research, research questions, research work hypothesis, research work objectives, the scope of the research work, the contribution of the research work, the novelty of the research work and thesis outline are presented in the chapter.

Chapter 2 – Literature Review: This chapter presents a literature review on base materials for (AlNB) composite, various thermal interface material with their growth techniques and respective thermal performances with LEDs. The theory of the sputtering deposition technique is also dealt with in the chapter.

Chapter 3 - Methodology: This chapter presents the detailed experimental procedures on the substrate preparation, materials growth, annealing and characterization techniques used throughout the research work.

Chapter 4 – Results and Discussion (Development and Analysis of AlNB Composites): This chapter dealt with the result and discussions of various characterization (phase structure, molecular structure, morphology and topography) carried out on the three configurations of AlNB composite.

Chapter 5 – Results and Discussion (Thermal and Optical Analysis of LED on Optimised AlN/B Composites): This chapter presents results and discussions based on thermal and optical characterization of LED with the developed solid thermal interface materials in the three configurations.

Chapter 6 – Conclusion and Recommendations for Future Work: This chapter portrays the main objectives, the summary and conclusion of the entire research work with recommendations for future research in the field; to improve AlN/B surface quality through the reduction of B impurities to a lower level and the use of Alumina substrate for better heat spreading.

CHAPTER 2

LITERATURE REVIEW

2.1 Introduction

The LEDs are becoming more efficient, affordable and energy saving, leading to lower energy cost and reduced peak demand, it offers improved service life at lower wattage with higher lumen power compared to conventional lighting technologies [3, 4]. The LEDs quality and output are on the rise progressively over the past years and it is expected to become the most dominant lighting technology of the future, surpassing all conventional lighting technologies driven by its edge with respect to service life, energy efficiency, versatility and lower cost [5, 6].

The luminous efficacy of LED is improving considerably in recent years, with an improvement of 6-8 lm/W per year since 2010 following the (Haitz's law), which is measured in lumens per package [7, 23]. It can also be compared to the advancement made in Si integrated circuits where the so called “Moore’s law”, predicts the performance of Si integrated circuits to doubles approximately every 18 months [24, 25] and attaining 161 lm/W by 2023 based on SDS [7].

All light sources convert input electric power into radiant energy and heat in varied proportions as presented in Table 2.1. on the other hand, LEDs generate zero IR and UV but convert only 15%-25% or 45% of the input power into visible photons [10, 26], while about 75% or 65% is converted to heat. The accumulation of heat at the die of the LED leads to the rise in T_j and seriously challenging the performance, reliability and operational life of the LED (sometime to catastrophic failure). It is further reported

by Gordon (2007) [10], that a rise in T_j by (10-11) °C can reduce the operational life of the LED by 50% as shown in Fig 2.1 and causing a noticeable chromaticity shift which might lead to reduced market penetration [9,10, 27-29]. This scenario can be challenged and managed by good thermal management. However, various research work has been carried out in the past to mitigate the accumulation of heat at the die of the LED which is largely driven by thermal path, ambient temperature and driving current through thermal management [53-63].

Table 2.1 Light Source with Approximate Input Power Conversion to Heat and Radiant Energy [10]

	Incandescent (60W)	Fluorescent (linear)	Metal Halide‡	LED
Visible Light	8%	21%	27%	15-25%
IR	73%	37%	17%	~ 0%
UV	0%	0%	19%	0%
Total Radiant Energy	81%	58%	63%	15-25%
Heat (Conduction + Convection)	19%	42%	37%	75-85%
Total	100%	100%	100%	100%

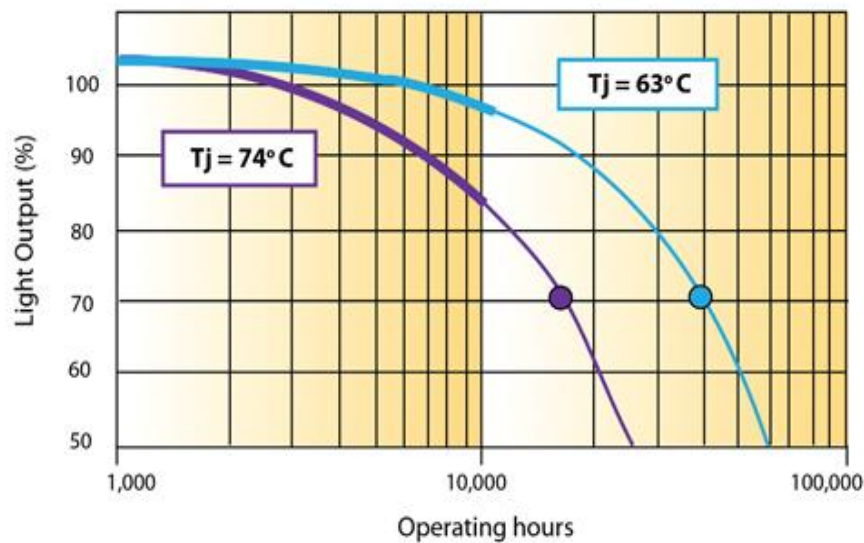


Figure 2.1 Useful Life of High-Power LED at Different Operational Temperatures [30]

2.2 Thermal Management

Drive current, thermal path, and ambient temperature are the three major influencers of T_j in solid state devices. The higher the applied current density, the higher the heat to be generated at the die. However, to maintain the expected luminous flux, operational life and color, the accumulated heat is expected to be mitigated away from the die by any or all of the known heat transfer phenomena (conduction, convection and radiation). On the other hand, the operational temperature needs to be maintained within safe limits as dictated by the data sheet of the LED and also the quality of the thermal path from the junction to ambient must be improved [10].

To mitigate the accumulated heat at the die and surroundings of the LED effectively, an efficient thermal path must be established between the LEDs' chip and the ambient by conduction. The heat flow path of the golden dragon LED is indicated in red arrow and illustrated with one dimensional R_{th} model in black at the right side of Fig 2.2 which is akin to an electrical circuit with heat source (Q) interchanged by current source, the heat flow by current (I), the temperature by voltage (V), and the (R_{th}) by resistor (R) in series.

The T_j , the R_{th} or most appropriately the Z_{th} and operational temperature are the three basic parameters considered by current researchers and industries in evaluating thermal performance of LED [31]. The use of Z_{th} to determine the heat flow path's ability to transfer heat across the LED package effectively cannot be over emphasize, because Z_{th} take into this consideration the sum of material's resistance and all contact resistances involve from die attach to heat sink as well as all possible defects within the grown material [31].

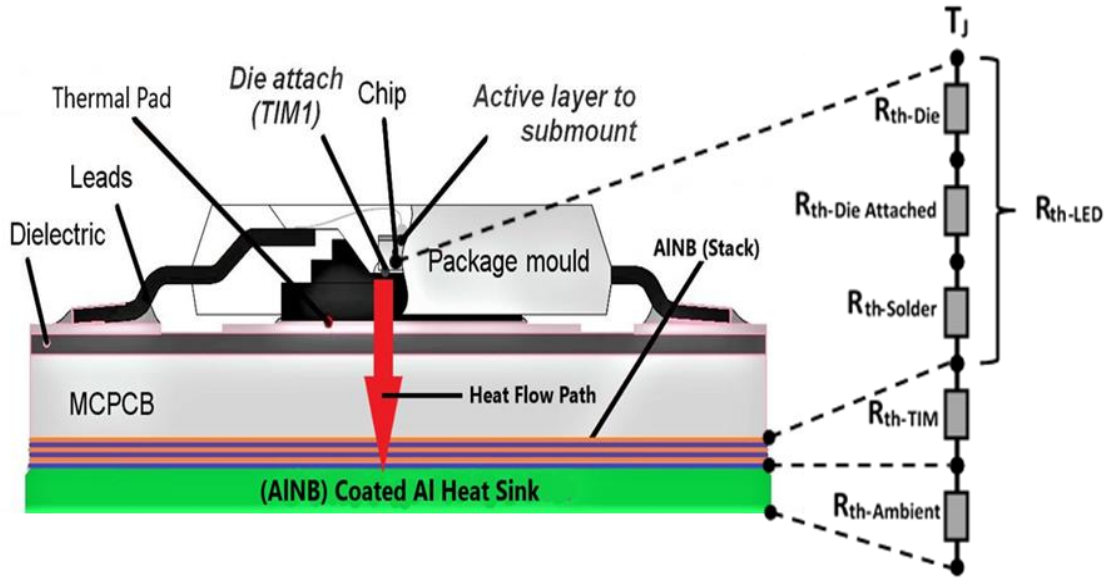


Figure 2.2 Heat Flow Path with One Dimensional R_{th} Model for the Golden Dragon LED

For successful thermal management of solid-state devices to attain reliability, higher flux and better operational life, various researchers proposed two major heat mitigation approach such as active and passive system. The active system is more effective but with higher cost and making the system bulky due to the introduction of fan and additional operational power requirement to drive the fan, on the other hand, it is more desirable to operate the passive system considering its simple structure and lower cost of production and maintenance [11].

However, one of the biggest challenges in the passive thermal path system is the presence of uneven contact points and gaps between the LED package and the heat sink surface largely due to roughness surfaces of the contacting bodies and occupied by high R_{th} air, the presence of air will increase R_{th} between the surfaces thus, interrupting the heat transfer [12, 13]. Thermal path improvement in the passive system is achieved through the surface filling of heat sink with low R_{th} materials in a form of pad, grease,

or solid thermal interface material (TIM) for the total or partial displacement of air in the gaps between the sink and LED surfaces as illustrated in Fig 1.3.

2.2.1 Solid thermal interface Material

STIM is a material with better thermal capabilities such as high conductivity, low R_{th} and or Z_{th} which could be considered as a crucial part of efficient thermal path for solid-state devices. It is expected to reduce junction-ambient R_{th} greatly which will lead to mitigation of elevated junction temperature, however the reduction in both R_{th} and T_j will improve the performance and reliability of the device [56]. The STIM is usually inserted in between the solid-state device (LED) as the heat source and heat sink in order to fill and or treat gaps, waviness, roughness and voids of two contacting surfaces as shown in Fig 2.3 to enhance heat dissipation from LED to ambient [32-34].

On the other hand, addition of thicker STIM in the package will increase the total R_{th} between the device and heat sink, thus the need to use STIM with higher thermal qualities and lower thickness to fill and eliminate minor surface defects (gaps) and dissipate heat to improve the thermal path cannot be over emphasized [35-38]. As reported by Jens et al.[33], Fig. 2.3 shows the R_{th} across the thermal joint comprising of three individual resistances in series, the effective R_{th} is given by Equation 2.1 helps to correlate the relationship between R_{th} and thermal conductivity of the material.

$$R_{th} = R_{contact\ 1} + R_{cond} + R_{contact\ 2} \quad (2.1)$$

Where $R_{contact\ 1}$ is the contact resistance between the lower surface and the TIM, $R_{cond} = BLT/kTIM$ is the bulk resistance of the TIM layer and $R_{contact\ 2}$ is the contact resistance between the TIM and the upper surface.

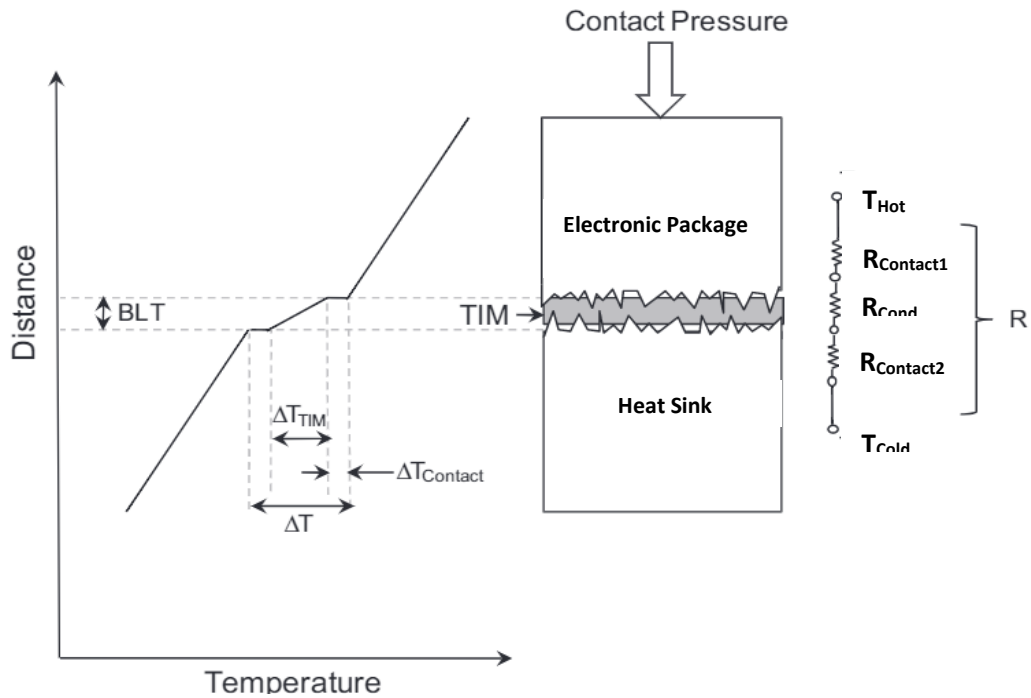


Figure 2.3 Schematic Representing a Real TIM and Associated Temperature Distribution with Resistor Model [33]

There exist various thermal interface materials in the market, including and not limited to phase change materials, grease, thermal paste, putties as well as polymer-based such as epoxies and silicones [32, 33, 39 - 55] though with some demerits, such as pump-out or dry-out of the material also paste squeezing and crack propagation at higher operational temperature [51].

2.2.2 Influence of thermal interface materials on heat mitigation

Previous literatures in the field of thermal management of LEDs are indicating a good reduction in R_{th} as well as T_j for effective heat mitigation based on various thermal interface materials mostly (oxides and nitrides) as presented in Table 2.2

Table 2.2 Summary of Previous Works in Thermal Resistance and Junction Temperature Reduction for Grown TIMS from Literatures

Author/Year	Method	Substrate	TIM	Current	ΔR_{th} K/W	ΔT_j °C
Shanmugan et al. (2014)	RF Sputter	Al	BN	700	1.92	2.97
Ong et al. (2015)	RF/DC Sput	Cu	B/AlN	700	1.43	3.37
Shanmugan and Mutharasu (2018)	CVD	Al	B/AlN	700	2.2	4.47
Shanmugan and Mutharasu (2016)	CVD	Al	B/AlN	700	3.25	3.22
Lim et al. (2017)	RF Sputter	Cu	Al ₂ O ₃	700	5.28	12.28
Jamaludin et al. (2016)	CVD	Al	Al ₂ O ₃	700	5.05	3.43
Muralidharan et al. (2020)	Anodization	Al	AAO-np	700	14.53%	14.87 %
Shanmugan et al. (2016)	Sputtering	Cu	ZnO	700	2.4	6.35
Shanmugan et al. (2013)	RF Sputter	Al	ZnO	700	3.85	7.46
Jamaludin and Shanmugan (2018)	CVD	Al	ZnO	700	2.14	4.80
Idris and Shanmugan (2020)	Spin Coating	Al	MgO	700	3.86	18.92

From the thermal resistance and junction temperature reductions obtained in previous literatures presented in Table 2.2, it shows a relatively good reduction in both R_{th} and T_j based on various TIMs, substrates and deposition techniques at current density of 700mA. Only two literatures were observed to have reported the reduction in T_j beyond 10°C which is the desired range for improving the thermal performance of LEDs for longevity, thus, the need to grow a robust material to attain higher reduction in T_j at higher current density and higher ambient temperature cannot be over emphasized.

2.3 Overview of Base Material (BN) Growth

Cubic Boron nitride (*c-BN*) thin films is a group III-V ceramic compound with a wide bandgap of ~ 6.2 eV which have receive reasonable attention due to its hard sp³-bonded diamond-like phase with a cubic zinc blend structure with unique and outstanding mechanical, thermal, electrical, and optical properties. Mechanically, the hardness of *c-BN* is believed to be in the range of about 4500 kg/mm² based on Vickers hardness test [64], making it the second hardest after diamond with low density. It is thermally stable with high melting point and excellent thermal conductivity up to 1300 W m⁻¹ K⁻¹ translated into low thermal resistance R_{th} , it also possesses high temperature resistance >2950 °C at inert atmosphere and high breakdown dielectric strength, making it a high-temperature dielectric with high electrical resistivity $\sim 10^{10}$ Ω cm. *BN* is a potential thermal TIM for thermal management application in optoelectronic devices at harsh environments. Optically *c-BN* is a transparent material with wide band gap and good transmittance over a wide spectral range from UV to visible, for application in optical instruments as emitters and UV detectors. [64-70]

Its very low reaction to ferrous metals and high resistance to oxidation at elevated temperatures is also making it very attractive in hard, protective coatings for tribological applications when compared to diamond. *c-BN* is thermally stable with high melting point and excellent thermal conductivity as well as low R_{th} for possible application as interfacial layers for thermal management in optoelectronic devices. Optically *c-BN* is a transparent material with wide band gap and good transmittance over a wide spectral range from UV to visible, for application in optical instruments as emitters and UV detectors. Furthermore, it is a good dielectric material with high electrical resistivity for applications in electron field emitters, high temperature electronic devices and as high-temperature dielectrics. [64-70]

. *c*-BN films deposited by physical vapor deposition (PVD) suffer from poor adhesion and cracking, whereas BN films deposited by chemical vapor deposition (CVD) might result in a mixture of *h*-BN, *t*-BN, and *c*-BN phases [70]. However, Post-deposition annealing is used to enhance the material structure, control surface roughness and eliminate intrinsic stress [12]

Various techniques such as RF/DC Magnetron sputtering deposition [64-66, 68], Pulsed laser deposition (PLD) [70, 71], Electron beam evaporation [72], Ion beam assisted deposition (IBAD) [73] and chemical vapour deposition (CVD) [70] were used to grow *c*-BN on variety of substrates.

2.3.1 Physical vapour deposition (PVD) techniques

Otano-Rivera et al. [74] and Bewilogua et al. [75] reported that Cubic boron nitride films were successfully prepared on *Si* (100) substrates with high-pressure RF reactive magnetron sputtering, using a *h*-BN target in pure *Ar* atmosphere. With the aid of the phase regulation of the applied RF voltages to the target and substrate electrodes and the magnetic field, the deposited thin films showed improved low roughness, homogeneity, purity, hydrophobicity, and nano-crystallinity [64-68]. While, In Pulsed laser deposition (PLD) technique, Polycrystalline *c*-BN films have been prepared at room temperature with the fraction of cubic material present in the deposited films depending on the laser energy density, the highest percentage occurs at an energy density of 2.4 J cm^{-2} . *c*-BN films prepared in *Ar* rich plasma show poor adhesion to *Si* (100) substrates, while the one prepared in pure N_2 plasma is maintained for more than 5 months without getting degraded [70, 71].

On the other hand, Monorama et al. [72], reported the growth of *c*-BN with electron beam evaporation where boron is evaporated in a graphite crucible and a tungsten filament was used to activate the nitrogen N₂ gas directed on the filament using a thin stainless-steel tube. A DC supply was used to heat the tungsten filament between the boron source and the substrate, at a substrate temperature of 400°C and nitrogen gas was introduced into the reaction chamber and directed onto the tungsten filament by the chamber whose pressure was increased to about 1.0x10⁸ Pa. The evaporation of Boron is carried out using an electron beam of energy 5 keV and current 100 mA, however, an estimated 1 mm thick cubic polycrystalline *c*-BN (95%) films were grown by this method.

The IBAD offers the advantage of control of all decisive deposition parameters, especially the ion energy, ion flux, and ion/boron ratio. Deyneka et al. [73] reported that a two-stage preparation process is applied to grow *c*-BN films on Si substrates in an IBAD system. At first stage a 50-nm thick *c*-BN seed layer was grown at a medium substrate temperature followed by growth at a higher substrate temperature of 800°C to enhanced the total momentum per boron atom in order to grow *c*-BN on top of the seed layer. However, a significant improvement in the crystalline quality was observed for the *c*-BN films accompanied by a considerable stress relaxation.

2.3.2 Chemical vapour deposition (CVD) techniques

Using the Chemical Vapour Deposition CVD technique, cubic Boron nitride (*c*-BN) films were grown on nickel substrates by hot-filament assisted RF plasma chemical vapour deposition (CVD) [76]. Ma et al. reported that the growth of BN films by hot filament assisted CVD strongly depended on the filament temperature leading to the formation of stoichiometric films with *c*-BN content of over 80% grown at temperatures

from 200 to 220°C. Further increase in temperature beyond this range leads to dramatic decrease in the c-BN content in the resulting films [70 - 76] the researcher went ahead to deposited c-BN thin films on different substrates (*Si*, *Ni*, *Ni-coated Si*, and stainless steel) by a hot filament assisted RF plasma chemical vapour deposition CVD.

Furthermore, Carreno et al. [77] prepared Boron nitride films with structures exhibiting a mixture of amorphous and hexagonal crystalline phases and even showing the onset of a cubic phase by the 13.56 MHz radio frequency PECVD technique in a capacitively coupled reactor with appropriate gaseous mixtures of nitrogen (N_2) and diborane (B_2H_6). The deposition temperature range was maintained from 200-500°C while the flow of gases was controlled by mass flow controllers. The RF power density and the (N_2)/ (B_2H_6) flow ratio is observed to have marked effect on the structure of the films where the hexagonal crystalline fraction decreased with increasing RF power densities and flow ratio values, however, the highest temperature and processing parameters values led to the formation of the cubic phase.

2.4 Overview of Base Material (AlN) Growth

2.4.1 Significance of AlN

aluminium Nitride (*AlN*) is a group III-V ceramic compound with a wide bandgap of ~6.2 eV [78]. It has remarkable physical and chemical properties which are adored by researchers in the field of optoelectronics and thermal management applications. It has inherent high thermal conductivity (260-600 $W.m^{-1}.K^{-1}$) compared to hexagonal aluminium nitride [14, 21], low R_{th} , low Z_{th} and low thermal expansion coefficient close to silicon with hardness of (40–50 GPa). It also possesses high thermal stability in air ~1000°C, high breakdown dielectric strength making it a good electrical